Assessment of Miscible Injection into a Basin Field in Kazakhstan: A Comparative Study of Hydrocarbon Gases, Nitrogen, and Carbon Dioxide

Bolatbek Khusain
D.V. Sokolsky Institute of Fuel, Catalysis and Electrochemistry, Almaty 050010, Kazakhstan
b.khusain@ifce.kz

Alexandr Logvinenko
Kazakh Institute of Oil and Gas, Almaty 050000, Kazakhstan
a.logvinenko@king.kz

Abzal Kenessary
Kazakh Institute of Oil and Gas, Almaty 050000, Kazakhstan
a.kenessary@king.kz

Ranida Tyulebayeva
Kazakh Institute of Oil and Gas, Almaty 050000, Kazakhstan
r.tyulebayeva@king.kz

Jamilyam Ismailova
Satbayev University, Almaty 050000, Kazakhstan
j.ismailova@satbayev.university

Dinara Delikesheva
Satbayev University, Almaty 050000, Kazakhstan
d.delikesheva@satbayev.university (corresponding author)

Received: 21 January 2025 | Revised: 16 April 2025, 22 April 2025, and 11 May 2025 | Accepted: 15 May 2025

 DOI: https://doi.org/10.48084/etasr.9826

ABSTRACT

This research investigated the miscible gas injection for Enhanced Oil Recovery (EOR) in a carbonate reservoir in Kazakhstan. Five mixtures, each containing varying percentages of methane, ethane, propane, carbon dioxide, and nitrogen, were studied to determine their Minimum Miscibility Pressure (MMP) values through PVT_i and slim tube tests. Among them, mixtures #2 (CH_4 and C_3H_8) and #4 (pure CO_2) exhibited the best performance, with mixture #2 achieving the lowest MMP value, while CO_2 showed the best miscibility at lower pressures and the option of potential carbon sequestration. Most of the results were supported by slim tube experiments, compositional simulations (Eclipse), and phase behavior analysis using Gibbs triangles and ternary diagrams. The study contributed to the EOR research by incorporating multi-component gas evaluation and advanced phase visualization, thereby filling the gaps by previous works focused on single gases. The key findings emphasized the need to balance the technical efficiency, environmental sustainability, and operational viability in gas selection, providing critical insights for optimizing the EOR strategies in similar reservoirs.

Keywords-carbon dioxide; phase diagram; minimum miscibility pressure; PVT

I. INTRODUCTION

In petroleum engineering, the efficient extraction of oils from reservoirs remains a critical challenge. As an oil field matures, the natural pressure that drives it to the surface diminishes, making the removal process even more difficult, further resulting in uncovered oil parts [1].

Miscible gas injection, an EOR technique, has been developed to address this challenge. It involves the injection of a solvent into the oil reservoir to mix with the initially present oil. Different reagents, like hydrocarbon gases, carbon dioxide, and nitrogen, are utilized increasing the oil's volume while reducing its viscosity, further improving its mobility, maintaining the reservoir pressure, and in some cases, achieving miscibility with the oil [2-5]. The carbon dioxide, used in the vaporizing gas drive method, is effective in extracting petroleum fractions due to its lower required mixing pressure compared to hydrocarbons. On the other hand, the nitrogen employed in the condensing gas drive method, achieves miscibility by the evaporation of light oil fractions.

Beyond improving the oil recovery, the miscible gas injection also offers environmental benefits. For instance, the use of carbon dioxide can lead to a reduction in the Greenhouse Gas (GHG) emissions as it can be sourced from industrial emissions, effectively sequestering it underground instead of releasing it into the atmosphere. Similarly, nitrogen does not contribute to GHGs due to its nature (inert gas).

This research investigates the effectiveness of CO_2 flooding for oil recovery, focusing on the influence of factors, like the oil composition, pressure, temperature, and asphaltene content.

II. MATERIALS AND METHODS

A. Field Area

Sedimentary rocks are the primary geological formations for hydrocarbon accumulation. They consist of subgroups, like carbonate (e.g., dolomite and limestone) and siliciclastic (e.g., sandstones and conglomerates) rocks. Carbonate reservoirs are often chosen due to their significant oil reserves, with structures, like reefs and dolomites. Both types of rocks have different responses to the acid treatments, affecting the filtration and volume properties. The carbonate layers can have a high oil content, while siliciclastic rocks are common with porosity around 20% and lower permeability.

The oilfield studied in this research dates to the Upper-Proterozoic period, situated near other producing fields. The productive zones are located in the southwestern portion of a geological platform composed of a crystalline base and sedimentary cover formed during the Riphean and Vend-Devonian periods. The geological structure consisted of metamorphic formations from Archean and Proterozoic eons, as well as sedimentary layers from Proterozoic and Paleozoic eras. The Riphean deposits contained effective horizons with carbonate and siliciclastic rocks, featuring simple and dual porosity. The productive horizon was primarily in Riphean dolomites, with additional pores, fractures, and caverns formed through processes, like paleohypergenesis.

B. Methods

1) Geological Model Construction in Petrel

A comprehensive geological model called Petrel was developed in order to obtain vital information about the reservoir's structure, properties, and inherent characteristics [6]. The process employed a rich set of input data, incorporating both the original data and the outcomes of comprehensive interpretations. The original data included key elements, such as locations, logging data, tracer studies, production and injection records, core studies, and seismic data. On the interpretation front, the results from seismic surveys, core analyses, stratigraphic breakdowns, structural assessments, fluid contact sampling, trends, and statistical information on analogs were combined. Elastic properties, such as acoustic impedance and density, were derived from seismic data through the application of inversion methods. These parameters are essential for understanding the subsurface characteristics and ensuring the accuracy of the geological interpretations.

2) PVTi Experiment for Gas Injection

Pressure-Volume-Temperature (PVT) experiments through a specialized PVT_i tool (Eclipse) were conducted to analyze the response of the reservoir sample to the gas injection under varying pressure, temperature, and volume conditions [2, 3].

3) Slim Tube Simulation

The slim tube experiment, using Eclipse 300, was employed to determine the MMP-the pressure at which injected gas achieves maximum miscibility with the reservoir fluids, thereby optimizing the recovery efficiency. This simulation involved the integration of the geological model from Petrel, PVT_i experiment results, and other relevant data.

The process involved gradual increments in pressure, continuing until a discernible improvement in oil recovery was observed. This point of enhanced recovery signified the attainment of miscibility, thus establishing the MMP [5-7].

The initial fluid composition in the reservoir is detailed in Table I.

TABLE I. OIL COMPOSITION IN THE RESERVOIR

Components	Z (Mole %)
H_2S	0.0006
CH_4	0.273
C_2H_6	0.4986
C_3H_8	0.0612
i-C_4H_{10}	0.015
n-C_4H_{10}	0.017
i-C_5H_{12}	0.0078
n-C_5H_{12}	0.0065
C_6H_{14}	0.0302
C^{7+}	0.0901

Pure gases, namely carbon dioxide (CO_2) and nitrogen (N_2), were utilized alongside specified hydrocarbon mixtures composed of methane (C_1), with either ethane (C_2) or propane (C_3) in varying percentages (Table II):

- Mixture #1: 30% Methane (CH_4) and 70% Ethane (C_2H_6),

- Mixture #2: 40% Methane (CH_4) and 60% Propane (C_3H_8)
- Mixture #3: 50% Methane (CH_4), 25% Ethane (C_2H_6), and 25% Propane (C_3H_8)
- Mixture #4:100% pure CO_2
- Mixture #5: 100% pure N_2

TABLE II. COMPOSITIONS OF INJECTED GAS

Components	#1	#2	#3	#4	#5
CO_2		-	-	100%	-
N_2	-	-	-	-	100%
CH_4	30%	40%	50%	-	-
C_2H_6	70%	-	25%	-	-
C_3H_8	-	60%	25%	-	-

The selection of gases was based on their technical feasibility for injection into Reservoir X and their known potential to achieve miscibility with the oil. Furthermore, these mixtures facilitated an advanced phase behavior analysis using Gibbs phase triangles and Cartesian ternary diagrams, which require distinct component differentiation for an accurate delineation of the miscibility envelopes.

The analytical component of this study primarily utilized Cartesian Ternary diagrams. These diagrams are theoretically derived from Gibbs triangular diagrams through a process of linear transformation. The two axes represent the mole fractions of two components: the light component (C_1) and the intermediate component (C_2). The fraction of the heavy component can be deduced by calculating the remaining portion of the system, using the right triangle's hypotenuse [8-11]. In the region where the concentration of the light component is highest, and the fractions of the others are lower, a single-phase gas state is observed. Conversely, the region with a predominance of the heavy component is indicative of a two-phase liquid state. Above the critical point, the diagram represents an area of supercritical fluid. It is important to note that the delineation of the two-phase region is subject to variation based on changes in the pressure and temperature values.

The lines of the constant compositions of both phases are called tie-line. The correlation between the total and phase concentrations is:

$$\begin{aligned} C_1 &= C_{1,gas}s + C_{1,oil}(1-s), \\ C_2 &= C_{2,gas}s + C_{2,oil}(1-s) \end{aligned} \quad (1)$$

where s is the gas saturation, and is calculated by:

$$s = \frac{C_1 - C_{1,oil}}{C_{1,gas} - C_{1,oil}} \quad (2)$$

Thus, for a three-component system the relation between methane and ethane is linear. In a tie-line diagram, the identical compositions of the liquid phase are identified by point A and the identical compositions of the gas phase are determined by point B. If the tie-line is placed in a higher region, then it will be hard to determine the difference between the liquid and gas compositions. The line touching the critical point is tangent to the two-phase envelope at the critical point.

The parameters of the tie-line can be presented as α and β, depending only on the phase composition. Specifically, parameter α is the tangent of the tie-lines, while β is the segment crossed by the tie-line on the vertical axes. For a three component system, from the relation between ethane and methane, it can be obtained:

$$\begin{aligned} C_2 &= aC_1 + \beta, \\ \alpha &= \frac{C_{2,gas} - C_{2,oil}}{C_{1,gas} - C_{1,oil}}, \\ b &= \frac{C_{2,oil}C_{1,gas} - C_{1,oil}C_{2,gas}}{C_{1,gas} - C_{1,oil}} \end{aligned} \quad (3)$$

The structure of fractional flow (F_1) can identify the behavior of the phase envelope process.

$$F_1 = \frac{Flowrate\ of\ component\ 1}{Total\ flowrate} \quad (4)$$

Using the total concentration of methane and parameter α, which is responsible for phase concentration, then methane can be replaced by F_2 in order to understand the structure of function F_1:

$$F_2 = \alpha F_1 + \beta \quad (5)$$

III. RESULTS AND DISCUSSIONS

A. Geological Model Construction using Petrel

Figure 1 illustrates the geological model from a frontal perspective.

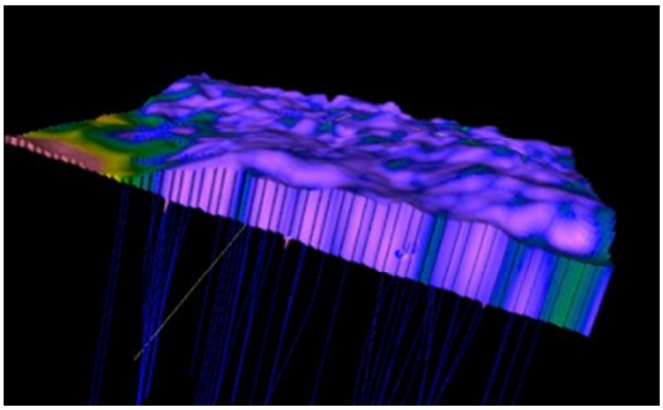

Fig. 1. The geological model (front view).

B. Minimum Miscibility Pressure

Table III presents the MMP calculated by PVT_i and slim tube experiments.

TABLE III. PVT_i EXPERIMENT FOR GAS INJECTION

Injection gases	MMP due to PVT_i (bar)	MMP due to Slim tube (bar)
CO_2	209.8095	190
N_2	419.3416	410
30% CH_4 and 70% C_2H_6	202.1816	220
40% CH_4 and 60% C_3H_8	189.2195	190
50% CH_4, 25% C_2H_6, and 25% C_3H_8	206.209	210

For CO_2, a noticeable difference between the two methods was observed. The PVT_i method estimated the MMP at 209.81 bar, whereas the slim tube method yielded a lower value of 190 bar. Similarly, N_2 also demonstrated a discrepancy, with MMP values of 419.34 bar in PVT_i and 410 bar in the slim tube method. In contrast, the gas mixture of 30% CH_4 and 70% C_2H_6 displayed an inverse relationship with the MMP at 202.18 bar in PVT_i and 220 bar in the slim tube method. For the mixture of 40% CH_4 and 60% C_3H_8, the MMP values were similar in both methods (189.22 bar in PVT_i and 190 bar in slim tube method). The more complex mixture with 50% CH_4, 25% C_2H_6, and 25% C_3H_8, showed a slight difference in the MMP values (206.21 bar in PVT_i and 210 bar in the slim tube method).

The differences in the MMP values between the PVT_i and slim tube methods can be attributed to the district nature of each approach [12-14]. The former technique is more theoretical, based on equations of state or other models that predict how gases behave under various pressures and temperatures. This method might provide an estimate that is more idealized and less reflective of the field conditions. Conversely, the slim tube method is more experimental and practical. It involves passing the gas through a long, slim tube filled with oil at varying pressures to determine the point at which miscibility occurs. This method is generally considered more accurate and closer to real-world conditions because it physically simulates the process [15, 16]. Based on the MMP values, the optimum gas for injection in the context of EOR can be determined by comparing the efficiency (lower MMP values) and practicality:

- CO_2 achieved a lower MMP making it efficient for miscibility with oil.
- N_2 revealed a higher MMP, which might limit its effectiveness.
- Gas Mixture #3 demonstrated MMP values that varied but were generally competitive with pure gases. Their specific compositions could be optimized for different reservoir conditions.

Considering these factors, CO_2 appeared as the most effective choice, enhancing its miscibility with oil under reservoir conditions [17].

The Ternary plots obtained in PVT_i Eclipse are presented in Figures 2-6 [18]. The green area represents the miscibility region indicating the conditions under which a single-phase system (gas-oil miscibility) can be achieved. The red line delineates the boundary of the two-phase region, where gas and oil remain partially immiscible.

Figure 2 illustrates the phase behavior of a mixture of reservoir oil with methane and ethane. Methane, being the lightest component, promoted the vaporization of the lighter fractions in the oil, while ethane contributed to the miscibility due to its higher molecular weight compared to methane. A miscibility region resulted (green area), highlighting the existence of a single-phase mixture. This zone represents conditions under which CH_4 and C_2H_6 are most effective in mixing with the reservoir oil, enhancing its recovery potential.

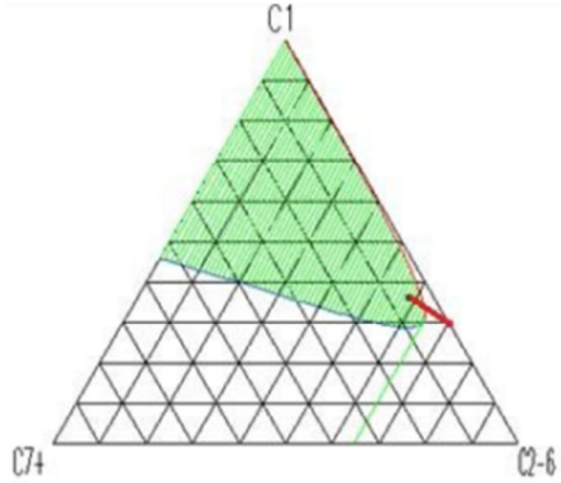

Fig. 2. Phase diagram of mixture #1.

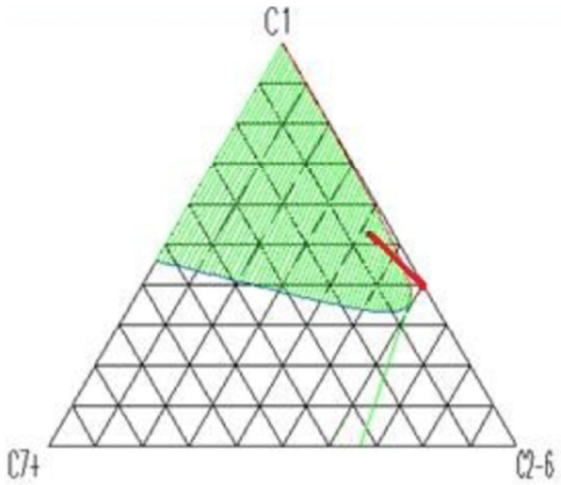

Fig. 3. Phase diagram of mixture #2.

Figure 3 depicts the phase behavior for a mixture of reservoir oil with methane and propane. The introduction of propane (heavier than ethane) expands the miscibility zone due to its higher condensation potential, allowing it to dissolve heavier fractions of the oil more effectively. The broader miscibility region (green area) suggested that mixture #2 can achieve miscibility at lower pressures than in mixture #1, making it more effective for EOR in certain conditions. The plot indicated that the presence of C_3 promoted the balance between vaporization (by C_1) and condensation (by C_3), leading to better oil solubilization.

Figure 4 represents the mixing behavior of the three-component system of methane, ethane, and propane with reservoir oil. This combination allowed for a wider miscibility region (green area). The presence of all three gases provided a balanced interaction, where methane promoted the vaporization of lighter oil components, ethane contributed to moderate miscibility properties, and propane enhanced the condensation of heavier components. As a result, the miscibility potential was maximized, making it ideal for EOR.

This finding implied that incorporating heavier gases or a combination of multiple gases with varying molecular weights could create more favorable conditions for mixing, improving the efficiency of oil recovery in depleted reservoirs.

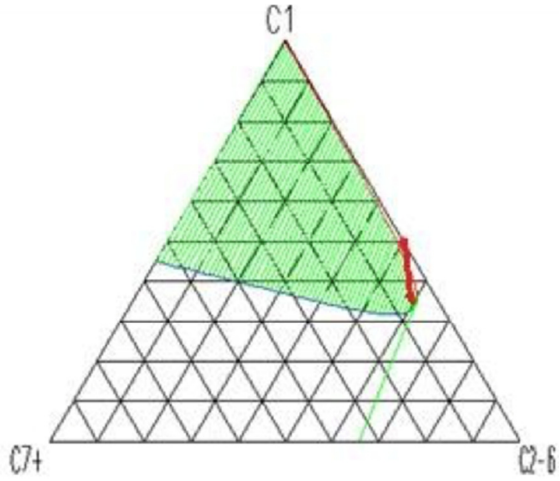

Fig. 4. Phase diagram of mixture #3.

The ternary plot in Figure 5 presented the phase behavior of a mixture of reservoir oil with CO_2. The green miscibility region indicated the conditions under which CO_2 could fully mixed with the reservoir oil, creating a single-phase behavior. This resulted in the reduction of interfacial tension, causing oil to swell and lowering viscosity, allowing more oil to be mobilized and produced. In Figure 6, the green area revealed a smaller miscibility region compared to CO_2, which may be attributed to the fact that nitrogen is less efficient than CO_2 in achieving miscibility at lower pressures.

Overall, these plots demonstrated the effectiveness of different gases in achieving miscibility with reservoir oil. Figure 5 was generally more efficient due to its lower MMP. N_2 injection, while also capable of recovering lighter hydrocarbons, required higher pressures to achieve miscibility, making it less efficient but still a viable option for EOR under specific reservoir conditions.

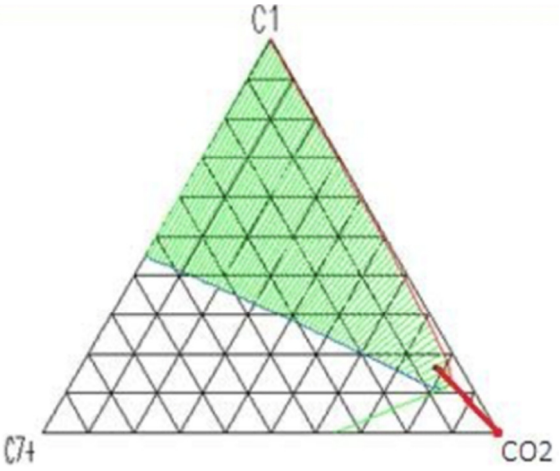

Fig. 5. Phase diagram of mixture #4.

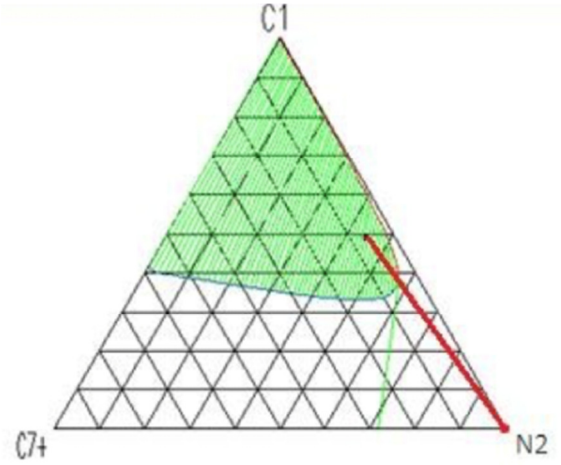

Fig. 6. Phase diagram of mixture #5.

C. Physico-Chemical Calculations

1) Mixture #2

The examination of the physico-chemical solution for the mixture #2 is presented in Figures 7-9, as it also yielded a low MMP value.

In Figure 9, BM is back shock, MN is Cs shock, and NA is the forward rarefaction way. The MN and BM shocks formed a sharp angle, because of the transport velocity changes.

Generalized fractional flow functions:

$$\mathcal{F}^1(s,a^0) = c_g^{(1)0}F^0(s) + c_{oil}^{(1)0}\left(1-F^0(s)\right) = 0.55F^0(s) + 0.36(1-F^0(s))$$

$$\mathcal{F}^1(s,a^{inj}) = c_g^{(1)inj}F^{inj}(s) + c_{oil}^{(1)inj}\left(1-F^{inj}(s)\right) = 0.4F^{inj}(s) + 0.28(1-F^{inj}(s))$$

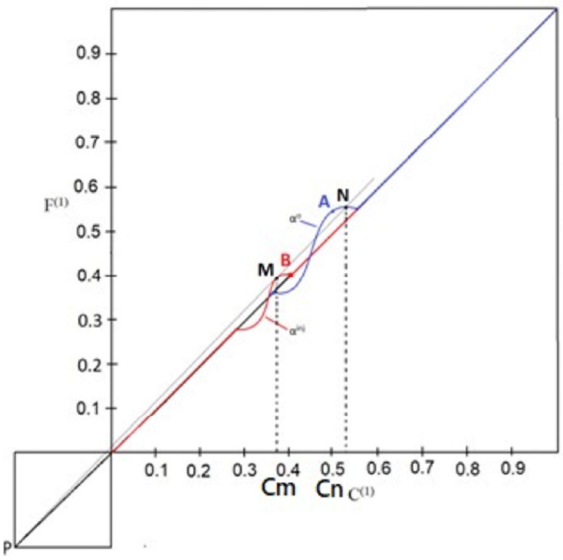

Fig. 7. Fractional flow versus concentration.

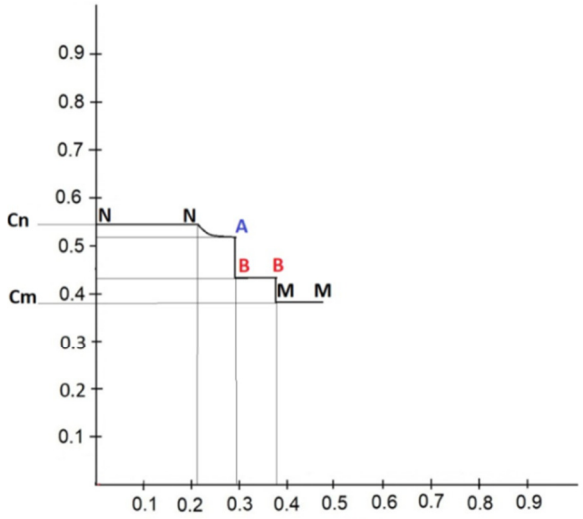

Fig. 8. Variation in space of the mixture composition in liquid phase.

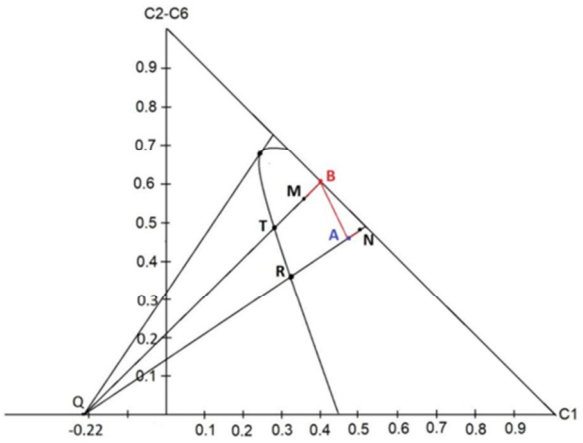

Fig. 9. Mixture #2 injection triangle and variation in space of the mixture composition in liquid phase.

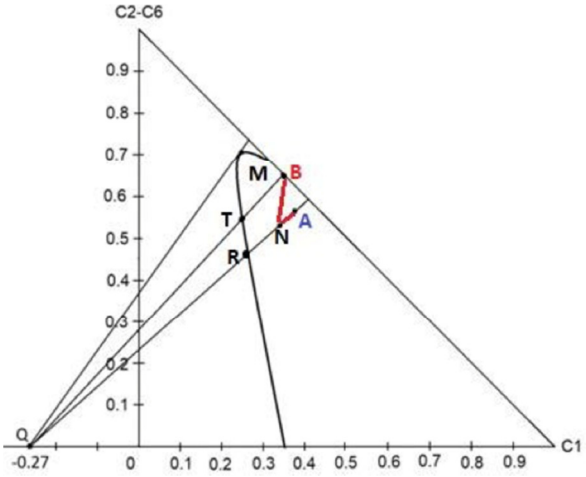

Fig. 10. Shock presentation in cartesian coordinates (mixture #1).

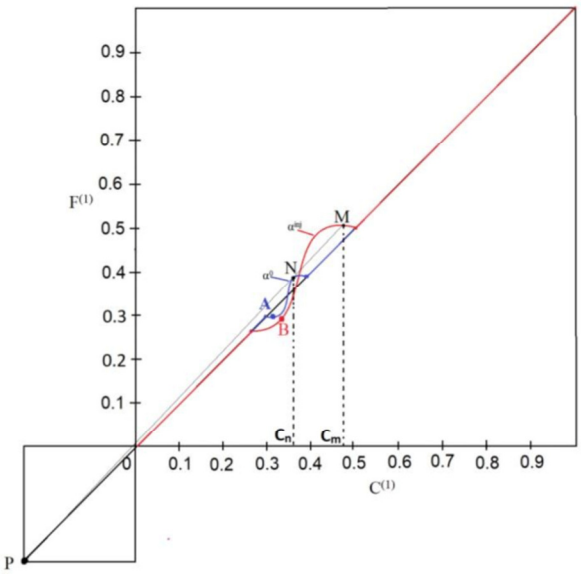

Fig. 11. Fractional flow versus concentration.

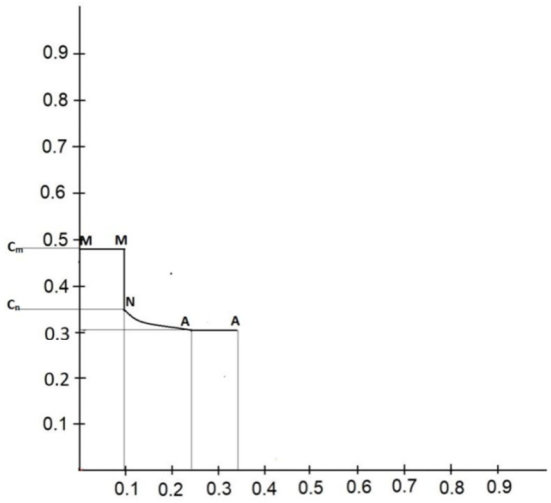

Fig. 12. Variation in space of mixture #1 composition in liquid phase.

2) Mixture #1

The physico-chemical solution of methane and ethane mixture #1 is illustrated in Figures 10-12. The B-B line is pure injection gas. M-M is the start of the displacement of oil by gas. Oil at this stage becomes lighter. N-A is the forward rarefaction wave, but displacement is still partial.

A-A shows the oil displaced by gas. This stage revealed how efficient the process was. During these shocks, sharp phase changes occurred: gas became heavier while oil lighter. The N-A indicated that the two phases achieved complete miscibility, and the vapor-liquid interface vanished.

3) Mixture #3

Figures 13-15 depict the physiochemical solution of mixture #3.

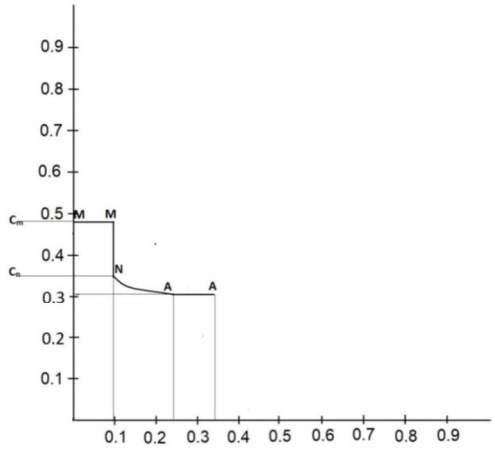

Fig. 13. Shock presentation in cartesian coordinates (mixture #3).

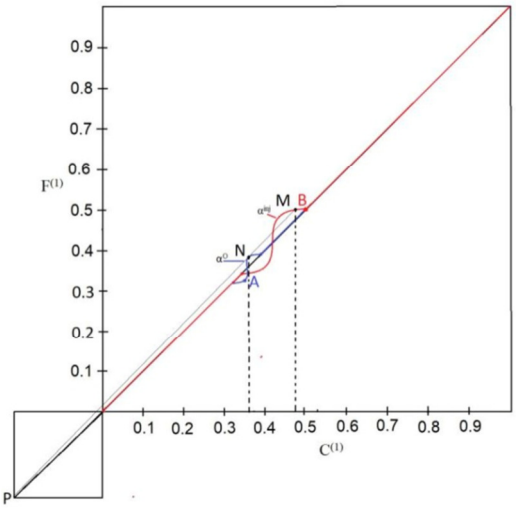

Fig. 14. Fractional flow versus concentration.

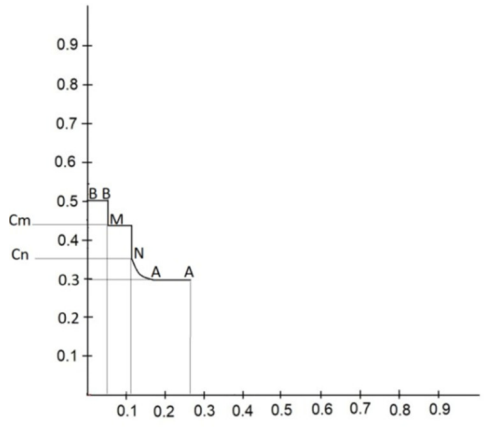

Fig. 15. Variation in space of the mixture composition in liquid phase.

Using the slim tube experiment, the MMP was determined by analyzing the recovery factor, as illustrated in Figure 16, where the recovery factor is plotted on the y-axis and the pressure on the x-axis.

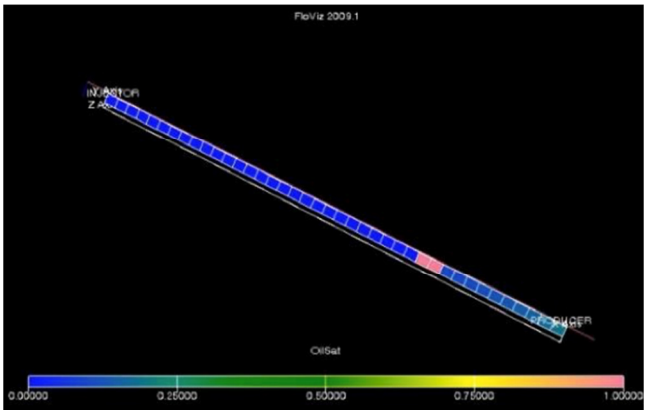

Fig. 16. Slim tube in FloViz.

The MMP values derived from both the recovery factor analysis and PVT_i studies were expected to agree, with only minor discrepancies, thereby validating the accuracy of the EOR predictions. Among the gases tested, CO_2 mixture #1 demonstrated a promising performance, indicating their effectiveness in EOR applications. In addition, their favorable outcomes were not solely based on MMP values and theoretical recovery potential, but considerations of the operational feasibility and cost-effectiveness were also incorporated. Figures 17-21 further compare the MMP results for CO_2, N_2, and various gas mixtures, understanding how different gases affect the oil recovery efficiency, particularly in terms of miscibility.

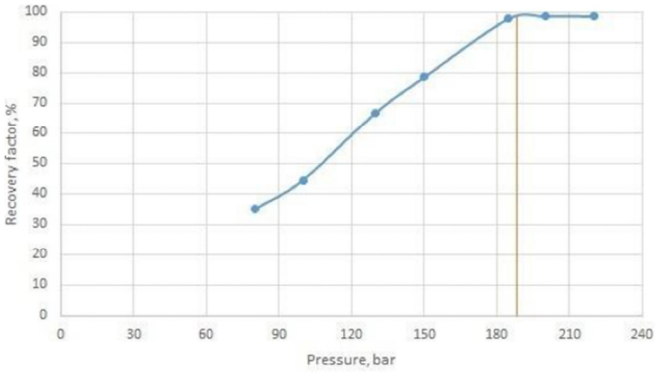

Fig. 17. MMP result for CO_2.

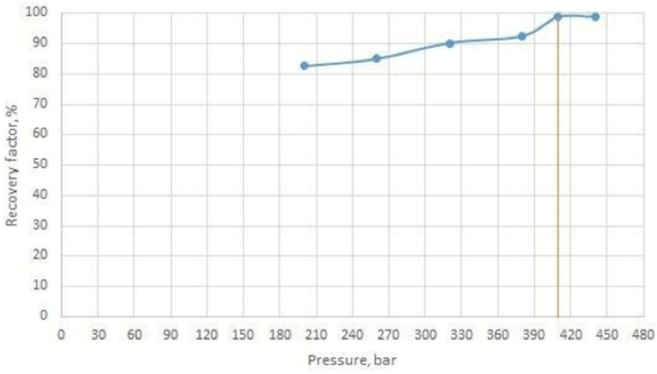

Fig. 18. MMP result for N_2.

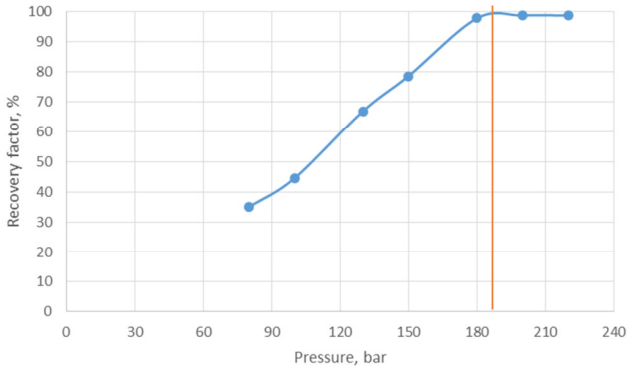

Fig. 19. Mixture #1 MMP result.

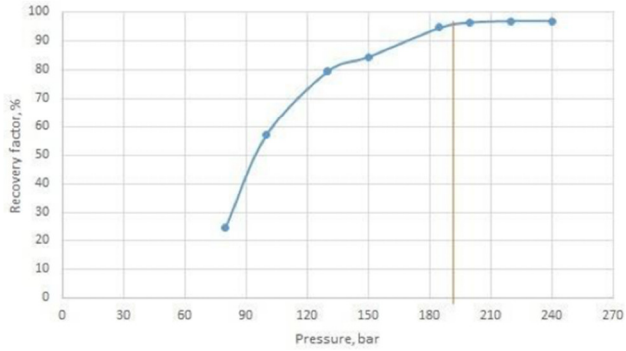

Fig. 20. Mixture #2 MMP result.

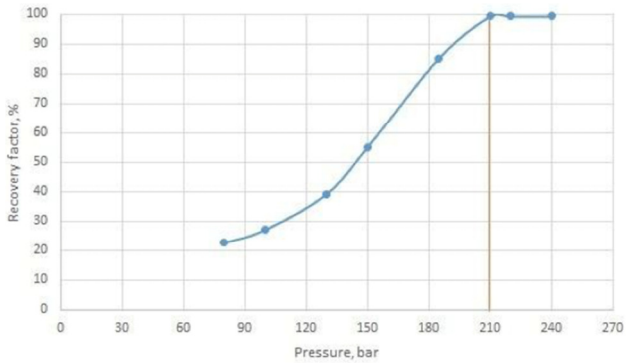

Fig. 21. Mixture #3 MMP result.

Table IV compares previous works on miscible gas injection in EOR, highlighting their shortcomings and illustrating the advances made in this study by employing a multi-gas, multi-component analysis, using robust simulation software, Gibbs phase triangles, and slim tube experimental validation.

The field oil production totals were also compared using three primary gases: nitrogen, carbon dioxide, and a selected mixed gas (Figures 22-24). The data indicated that the nitrogen injection resulted in the lowest total field oil production compared to both the CO_2 and mixed gas.

TABLE IV. COMPARISON TABLE

Study	Objective	Methods	Key findings	Shortcomings	Advancements in current study
[19]	Coupled CO2-EOR recovery and CO_2 storage in residual oil zones under Water-Alternating-Gas (WAG) flooding.	Compositional reservoir simulation incorporating molecular diffusion; scenario analysis with varied formation and operational parameters (e.g., permeability, WAG ratio, temperature, BHP).	Demonstrated the effectiveness of WAG-CO2 injection in maximizing oil recovery and CO_2 storage, highlighting the impact of reservoir and injection conditions on the overall performance.	Focused solely on CO2, did not explore alternative gases or experimental validation; site-specific conclusions may not apply universally. .	This study uses PVTi and slim tube comparison for multiple gases, offering broader insight into gas injection efficiency and miscibility behavior under different reservoir conditions.
[20]	CO2 flooding effects on shale oil recovery and residual oil distribution using NMR tracking.	NMR imaging of core flood tests (CO_2 versus water). Measured MMP and oil recovery by stepwise pressure increases (0.7–11 MPa) in mini-slim-tube experiments.	Demonstrated that CO2 flooding significantly enhances oil recovery in shale, with measurable MMP and distinct remaining oil profiles mapped by NMR.	Demonstrated that CO2 flooding significantly enhances oil recovery in shale, with measurable MMP and distinct remaining oil profiles mapped by NMR.	Provides empirical MMP data for multi-component gas mixtures, offering detailed insights on mixed gas efficiency and miscibility under real reservoir conditions.
[21]	To investigate the miscibility and EOR performance of CO2 injection in shale oil reservoirs.	Laboratory-scale coreflooding experiments combined with numerical simulation using CMG-GEM; analysis of phase behavior and oil recovery under different injection conditions.	CO2 injection improves oil recovery in shale reservoirs due to effective miscibility; higher injection pressure enhances recovery; diffusion and swelling are key mechanisms.	Focused only on CO2 as the injection gas.	Supports experimental insights into miscibility development in tight shale formations, offering practical implications for optimizing CO2-EOR in unconventional reservoirs.

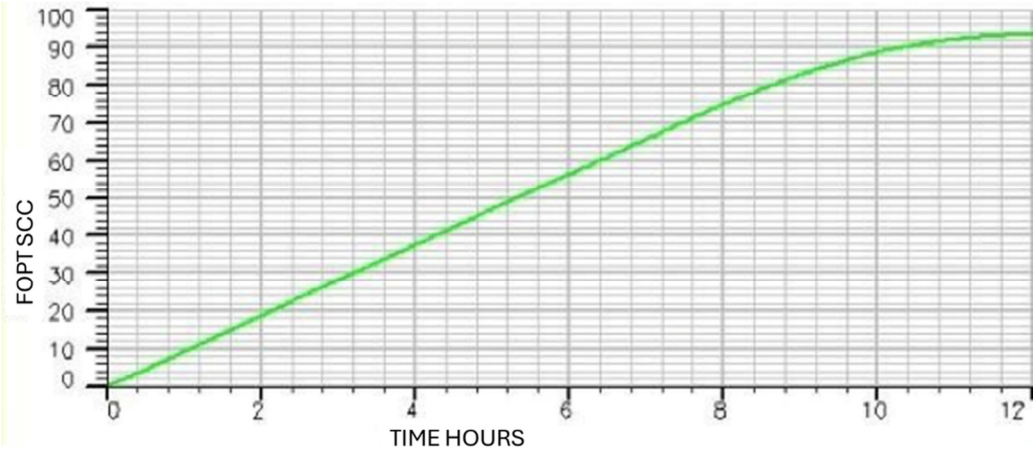

Fig. 22. CO_2 experiment field oil production total.

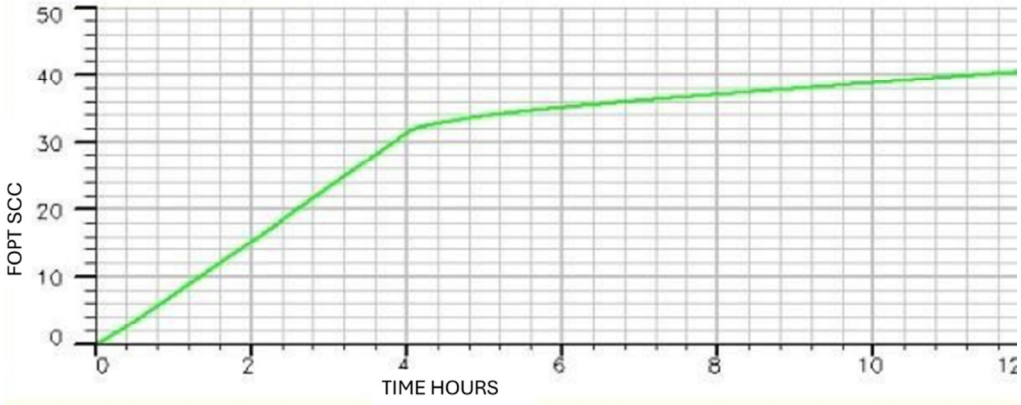

Fig. 23. N_2 experiment field oil production total.

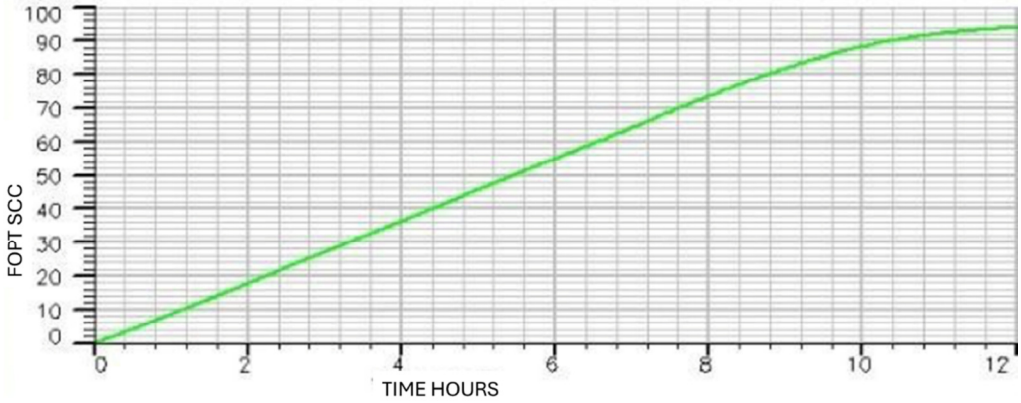

Fig. 24. Mixture #1 experiment field oil production total.

Additionally, this analysis revealed that the use of CO_2 in EOR not only aligned with the environmental considerations, but also competed effectively in terms of the oil production output. This suggested a dual benefit: the mitigation of GHGs emissions and the stabilization of efficient oil recovery rates. Such a strategy could be pivotal in the energy sector, where the balance between the environmental impact and resource extraction efficiency is critical. Since CO_2 and the mixed gas performed similarly, further research could explore optimal gas mixtures to enhance both efficiency and sustainability (Figures 25, 26).

D. Simulation Model in Eclipse

The Eclipse 300 and Petrel software were incorporated to assess various gas flooding processes in a geological model of a reservoir utilizing Petrel-generated grid parameters, porosity, permeability properties, and fracture data in the Eclipse model.

ECLIPSE 300, known for handling compositional changes, was apt for evaluating the chosen hydrocarbon gas mixtures [22]. Among them, mixture #1 and CO_2 were injected at 200 bar, while nitrogen required a higher pressure of 300 bars, indicating its high miscibility pressure. This aspect, along with the observed lower production profile of nitrogen in slim tube experiments, underscored the capital costs associated with these displacement processes, making them less frequently employed in practice.

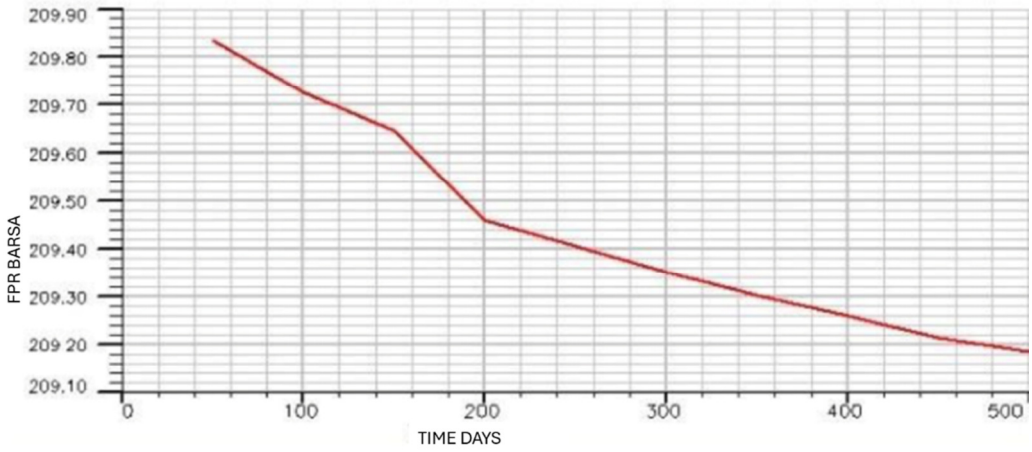

Fig. 25. Field pressure profile for mixture #1.

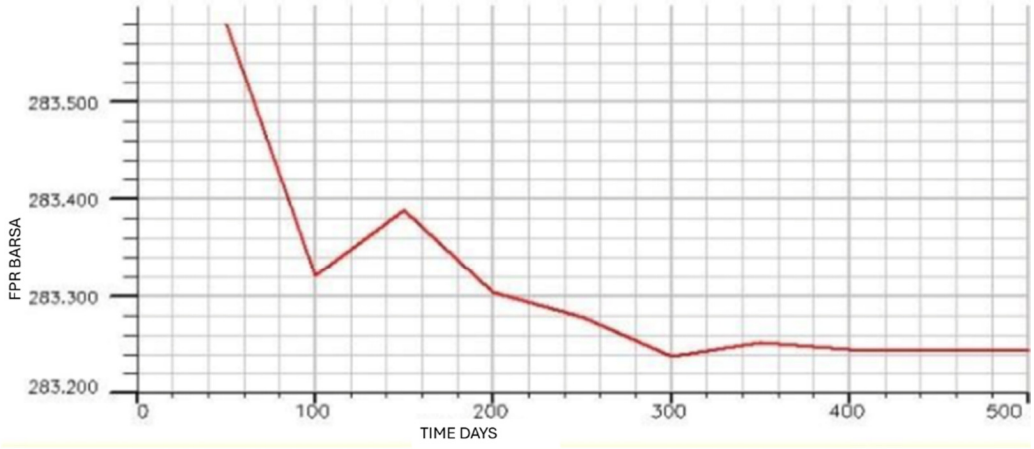

Fig. 26. Field pressure profile for mixture #4.

Figures 25-26 illustrate the pressure profiles versus time for mixtures #1 and #4, in order to understand how the pressure in an oil field changes over time with the injection of various gases. Each gas, due to its unique properties, will influence the field pressure differently. A steep pressure change might suggest a more effective displacement of oil by the injected gas, whereas a more gradual change could indicate less efficient displacement. The comparison across different gases can provide insights into which gas is the most effective under the specific conditions of the field.

IV. CONCLUSIONS

This study provided a comparative assessment of miscible gas injection strategies using carbon dioxide (CO_2), nitrogen (N_2), and selected hydrocarbon gas mixtures for Enhanced Oil Recovery (EOR) in a carbonate reservoir in Kazakhstan. Five gas formulations were investigated:

- Mixture #1: 30% Methane (CH_4) and 70% Ethane (C_2H_6)
- Mixture #2: 40% Methane (CH_4) and 60% Propane (C_3H_8)
- Mixture #3: 50% Methane (CH_4), 25% Ethane (C_2H_6), and 25% Propane (C_3H_8)
- Mixture #4: 100% Carbon Dioxide (CO_2)
- Mixture #5: 100% Nitrogen (N_2)

Among these, Mixture #2 and Mixture #4 demonstrated the most favorable performance in terms of miscibility and oil recovery. Mixture #2 had the lowest Minimum Miscibility Pressure (MMP) value while exhibiting excellent phase behavior and oil displacement efficiency, largely due to propane's strong condensation properties. Mixture #4 revealed similar advantages, with the added benefit of lower operational

pressure requirements and significant environmental potential through CO_2 sequestration.

The findings were validated through both slim tube experiments and compositional simulations using the Eclipse software, with miscibility zones visualized via Gibbs phase triangles and Cartesian ternary diagrams. The correlation between the simulation and experimental results confirmed the reliability of the current method.

This study also highlighted the novelty of integrating advanced phase behavior analysis with multi-component gas mixture evaluation in reservoir conditions. Unlike prior works that primarily focused on individual gases or lacked phase visualization tools, this research provided a complete understanding of the gas-oil interactions, offering practical insights for field application. Additionally, the comparative approach underscored the importance of not only evaluating the technical efficiency, but also considering the environmental sustainability and operational feasibility when selecting injection gases.

ACKNOWLEDGMENT

The research was funded by the Committee of Science of the Ministry of Science and Higher Education of the Republic of Kazakhstan (Grant No. BR21882241)

REFERENCES

[1] E. M. Mansour, A. M. Al-Sabagh, S. M. Desouky, F. M. Zawawy, and M. Ramzi, "A new estimating method of minimum miscibility pressure as a key parameter in designing CO2 gas injection process," *Egyptian Journal of Petroleum*, vol. 27, no. 4, pp. 801–810, Dec. 2018, https://doi.org/10.1016/j.ejpe.2017.12.002.

[2] E. A. Chukwudeme and A. A. Hamouda, "Enhanced Oil Recovery (EOR) by Miscible CO2 and Water Flooding of Asphaltenic and Non-Asphaltenic Oils," *Energies*, vol. 2, no. 3, pp. 714–737, Sep. 2009, https://doi.org/10.3390/en20300714.

[3] S. Chandra, P. A. Aziz, M. R. Naufal, and W. N. Daton, "Well Integrity Study for CO2 WAG Application in Mature Field X, South Sumatra Area for the Fulfillment as CO2 Sequestration Sink," *Scientific Contributions Oil and Gas*, vol. 44, no. 2, pp. 107–121, Aug. 2021, https://doi.org/10.29017/SCOG.44.2.587.

[4] V. S. Rios, L. O. S. Santos, F. B. Quadros, and D. J. Schiozer, "New upscaling technique for compositional reservoir simulations of miscible gas injection," *Journal of Petroleum Science and Engineering*, vol. 175, pp. 389–406, Apr. 2019, https://doi.org/10.1016/j.petrol.2018.12.061.

[5] H. Hao, J. Hou, F. Zhao, H. Huang, and H. Liu, "N_2 -foam-assisted CO_2 huff-n-puff process for enhanced oil recovery in a heterogeneous edge-water reservoir: experiments and pilot tests," *RSC Advances*, vol. 11, no. 2, pp. 1134–1146, 2021, https://doi.org/10.1039/D0RA09448J.

[6] M. A. Khashman and H. Shirazi, "3D Geological Modeling with Petrel Software: Estimating Original Oil in Place of Lower Cretaceous Y-Formation: A Case Study in a Selected Oilfield." Sep. 25, 2023, https://doi.org/10.21203/rs.3.rs-3345863/v1.

[7] A. A. Hamouda and S. Chughtai, "Miscible CO2 Flooding for EOR in the Presence of Natural Gas Components in Displacing and Displaced Fluids," *Energies*, vol. 11, no. 2, Feb. 2018, Art. no. 391, https://doi.org/10.3390/en11020391.

[8] L. W. Lake, *Enhanced Oil Recovery*. Hoboken, NJ, USA: Prentice Hall, 1989.

[9] M. Abdurrahman *et al.*, "Minimum CO_2 Miscibility Pressure Evaluation using Interfacial Tension (IFT) and Slim-tube Hybrid Tests," *ACS Omega*, vol. 8, no. 9, pp. 8703–8711, 2023, https://doi.org/10.1021/acsomega.2c08085.

[10] L. Yang, W. Rui, Z. Qingmin, Z. Yuanlong, F. Xin, and X. Zhaojie, "CO2-enhanced oil recovery with CO2 utilization and storage: Progress and practical applications in China," *Unconventional Resources*, vol. 4, Jan. 2024, Art. no. 100096, https://doi.org/10.1016/j.uncres.2024.100096.

[11] J. J. Sheng, "Enhanced oil recovery in shale reservoirs by gas injection," *Journal of Natural Gas Science and Engineering*, vol. 22, pp. 252–259, Jan. 2015, https://doi.org/10.1016/j.jngse.2014.12.002.

[12] M. Ding, M. Gao, Y. Wang, Z. Qu, and X. Chen, "Experimental study on CO2-EOR in fractured reservoirs: Influence of fracture density, miscibility and production scheme," *Journal of Petroleum Science and Engineering*, vol. 174, pp. 476–485, Mar. 2019, https://doi.org/10.1016/j.petrol.2018.11.039.

[13] S. Sakthivel, A. Adebayo, and M. Y. Kanj, "Experimental Evaluation of Carbon Dots Stabilized Foam for Enhanced Oil Recovery," *Energy & Fuels*, vol. 33, no. 10, pp. 9629–9643, Oct. 2019, https://doi.org/10.1021/acs.energyfuels.9b02235.

[14] F. Guo and S. Aryana, "An experimental investigation of nanoparticle-stabilized CO2 foam used in enhanced oil recovery," *Fuel*, vol. 186, pp. 430–442, Dec. 2016, https://doi.org/10.1016/j.fuel.2016.08.058.

[15] X. Zhou, Q. Yuan, Y. Zhang, H. Wang, F. Zeng, and L. Zhang, "Performance evaluation of CO2 flooding process in tight oil reservoir via experimental and numerical simulation studies," *Fuel*, vol. 236, pp. 730–746, Jan. 2019, https://doi.org/10.1016/j.fuel.2018.09.035.

[16] Y. Su *et al.*, "The Influence of Slim Tube Length on the Minimum Miscibility Pressure of CO2 Gas–Crude Oil," *Processes*, vol. 12, no. 4, Apr. 2024, Art. no. 650, https://doi.org/10.3390/pr12040650.

[17] N. Badrouchi, H. Pu, S. Smith, and F. Badrouchi, "Evaluation of CO2 enhanced oil recovery in unconventional reservoirs: Experimental parametric study in the Bakken," *Fuel*, vol. 312, Mar. 2022, Art. no. 122941, https://doi.org/10.1016/j.fuel.2021.122941.

[18] M. Hussain, F. Boukadi, Z. Hu, and D. Adjei, "Optimizing Oil Recovery: A Sector Model Study of CO_2-Water-Alternating-Gas and Continuous Injection Technologies," *Processes*, vol. 13, no. 3, Mar. 2025, Art. no. 700, https://doi.org/10.3390/pr13030700.

[19] B. Liu, J. Yao, and T. Sun, "Numerical analysis of water-alternating-CO2 flooding for CO2-EOR and storage projects in residual oil zones," *International Journal of Coal Science & Technology*, vol. 10, no. 1, Nov. 2023, Art. no. 73, https://doi.org/10.1007/s40789-023-00647-9.

[20] L. Fan, J. Chen, J. Zhu, X. Nie, B. Li, and Z. Shi, "Experimental Study on Enhanced Shale Oil Recovery and Remaining Oil Distribution by CO2 Flooding with Nuclear Magnetic Resonance Technology," *Energy & Fuels*, vol. 36, no. 4, pp. 1973–1985, Feb. 2022, https://doi.org/10.1021/acs.energyfuels.1c02982.

[21] M. M. A. Awan and F. U. D. Kirmani, "CO2 injection for enhanced oil recovery: Analyzing the effect of injection rate and bottom hole pressure," *Petroleum Research*, vol. 10, no. 1, pp. 129–136, Mar. 2025, https://doi.org/10.1016/j.ptlrs.2024.08.006.

[22] K. K. Ihekoronye, A. D. I. Sulaiman, M. B. Adamu, H. Usman, R. Z. Milton, and C. A. Ibrahim, "3-D Modelling and Simulation of a Reservoir for Surfactant-Polymer Flooding Using Eclipse Software," *Petroleum & Coal*, vol. 66, no. 2, pp. 691–701, 2024.